A MICRO MAGNETIC BEARING WITH A 2 MM-DIAMETER ROTOR AND ITS PERFORMANCE

Jiro Kuroki
Department of Mechano-Micro Engineering, Tokyo Institute of Technology, Yokohama, 226-8503, Japan
d03kuroki@pms.titech.ac.jp

Tadahiko Shinshi and Akira Shimokohbe
Precision & Intelligence Laboratory, Tokyo Institute of Technology, Yokohama, 226-8503, Japan
shinshi@pi.titech.ac.jp, shimo@pi.titech.ac.jp

Lichuan Li
Department of Electrical Machines, Xi'an Jiaotong University, 710049, Xi'an, China
lcli@mail.xjtu.edu.cn

ABSTRACT

A novel micro-magnetic bearing (MMB) with a 2 mm-diameter rotor is discussed. The MMB has a simple structure and consists of some mechanical parts and a permanent magnet. The rotor is supported by magnetic couplings generated by the permanent magnet and is stabilized by a one-axis-controller. The MMB for the 2 mm-diameter rotor was constructed, such that the rotor could be levitated without mechanical contact and which could rotate at 39,000 rpm. The static and dynamic characteristics of the MMB are evaluated. The measured magnetic stiffness in the passively controlled radial and angular directions was 4.7 N/mm and 2.7×10^{-2} Nm/rad, respectively. The total power consumption and copper loss without rotation were 20.4 mW and 17.2 mW, respectively.

INTRODUCTION

Magnetic bearings possess the advantages of being non-contact, non-friction and non-wear. Rotors supported by magnetic bearings can not only rotate at high speed, but can also be used in a vacuum or a liquid. Hence, magnetic bearings are employed in industrial applications such as turbo molecular pumps, flywheels and blood pumps. However, conventional magnetic bearings require many electromagnets and displacement sensors to control the multiple-degree-of-freedom available to the motion of the rotor, so much so that the bearings require complex mechanical and electrical systems. Also, the miniaturization of magnetic bearings has yet to be satisfactorily discussed. However, micro and non-contact bearings will be required in micro-turbines [1] and axial flow pumps for artificial hearts [2] because of the necessity for high speed, exceptional cleanliness and extreme durability. The use of MMBs may provide one of the solutions.

Some research into MMBs has already been reported. Kummerle et al. [3] presented an MMB using 5-degree-of-freedom (5-DOF). However, further miniaturization is difficult for this style of MMB because 5-DOF control using many displacement sensors and electromagnets is necessary. Reducing the number of actively controlled DOF may be one solution for further miniaturization.

Many papers have reported the passive stabilization of magnetic bearings. In order to realize passive magnetic bearings, magnetic couplings induced by permanent magnets are used. Yonnet [4,5] reported techniques for applying various magnetic couplings to magnetic bearings. Iwahara et al. [6] and Horikawa et al. [7] discussed one-axis-controlled magnetic bearings with the permanent magnets. However the magnetic bearings possess low magnetic stiffness because the magnetic flux from the permanent magnets does not form a magnetic closed loop. Also, the miniaturization of these types of magnetic bearings has not been discussed.

The Authors et al. [8] proposed a simple structure for an MMB that can be stabilized using only one-axis-control and realized an MMB for an 8 mm-diameter rotor. In the proposed MMB, the magnetic flux forms a closed magnetic loop and its structure is

simpler than those of magnetic bearings described previously. Hence, our MMB possesses high magnetic stiffness in the passively controlled directions compared with one of the same size without a closed magnetic flux and is suitable for miniaturization. However the MMB is not sufficiently small to be employed in micro applications.

In order to realize a further miniaturized MMB, we proposed a structure of the MMB for a 2 mm-diameter rotor [9] that was greatly simplified, not only in terms of machining and assembly of micro- and precision parts, but the number of mechanical parts was also reduced in comparison with previous designs of MMB [8]. Furthermore to increase the magnetic stiffness used to support the rotor in the passively controlled directions and to realize stable levitation using one-axis-control, the dimensions of the mechanical parts that affect the magnetic stiffness were investigated [9] using a finite element method.

In this paper, the MMB for the 2 mm-diameter rotor is fabricated and constructed, such that the rotor could be levitated without mechanical contact. The static and dynamic characteristics of the MMB are evaluated such as magnetic stiffness, rotational accuracy and power consumption.

PRINCIPLES OF THE MMB

A novel magnetic coupling was used to attempt to reduce the number of degrees of freedom for the rotor that need to be controlled, with the aim of miniaturizing the magnetic bearing, as shown in Figure 1. The structure of the MMB is much simpler than that of conventional 5-DOF controlled magnetic bearings, which normally include ten electromagnets and five displacement sensors.

The rotor consists of an aluminum shaft and a steel cylinder without laminations. The stator consists of a permanent magnet, two steel flanges and two ring-shaped coils connected serially. A displacement sensor is used to control the rotor motion along the Z-axis, as shown in Figure 1.

The magnetic flux from the permanent magnet (indicated by the solid line) works as a magnetic coupling on both sides of the steel cylinder, generating a restoring force and torque if the rotor shifts in the X or Y direction and/or rotates in the Θ or Φ directions from the balanced position. The magnetic couplings are generated between the precisely machined steel cylinder and the flanges such that the rotational accuracy is not affected by the accuracy of the conformation of the permanent magnet. However, without any control in the Z direction, the magnetic couplings generate an attractive force, causing the steel cylinder to stick to either side of the flanges. In order to realize a non-contact support for the rotor, the current through the coils is regulated, thus controlling the fluxes indicated by the dotted lines in Figure 1.

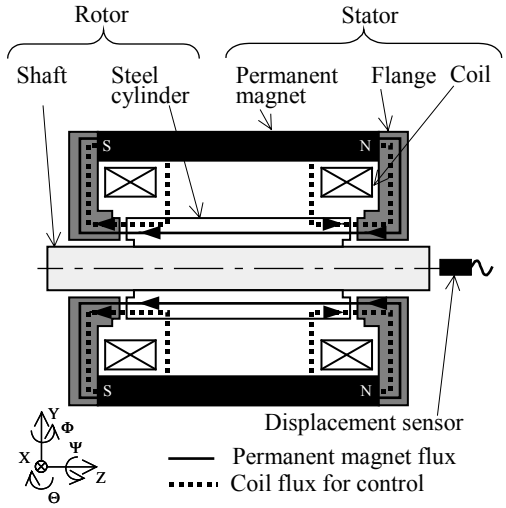

FIGURE 1: Schematic of proposed MMB

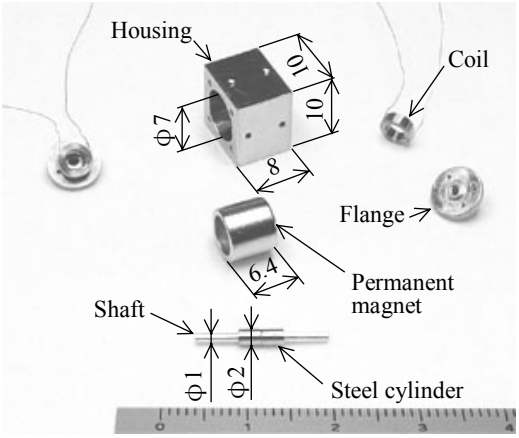

(a) Components of MMB

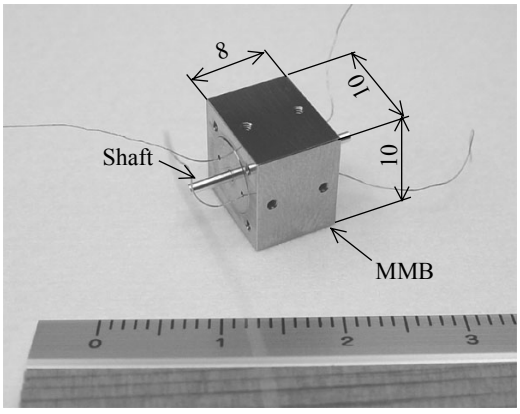

(b) Assembled MMB

FIGURE 2: Components and assembled MMB

FABRICATION

An MMB was fabricated and constructed as shown in Figure 2. All of the mechanical parts were fabricated using conventional machining processes. The edges of the steel cylinder and the pipe edges of the flanges (which work as magnetic couplings) were machined precisely in order to avoid the generation of burrs and to avoid chamfering, since experiments have shown that burrs and chamfering reduce the magnetic stiffness in the passively controlled directions.

The steel cylinder was glued to an aluminum shaft. One end face of the shaft, which is the target of the displacement sensor, was precisely machined. The mass of the rotor was 1.3×10^{-4} kg. There were 104 turns on the micro-ring-shaped coil. The diameters of the wire, the inner ring and the outer ring were 0.1 mm, 2.6 mm and 4.8 mm, respectively. A housing was used in order to assemble all parts. The dimensions of the housing, which was made from SUS316, were 8 mm×10 mm×10 mm. A hole of 7 mm-diameter was bored precisely through the 10 mm×10 mm surface. This had an allowable dimensional deviation of 8 μm and a tolerance of cylindricality of 5 μm because all the mechanical parts were assembled based on the inner surface of the housing. Any assembly error causes a reduction in magnetic stiffness and, in the worst case, results in contact between the rotor and the stator.

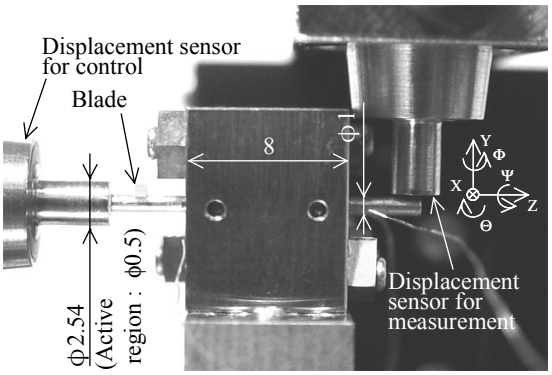

FIGURE 3: Experimental setup

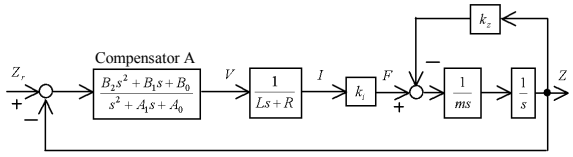

(a) Control system A

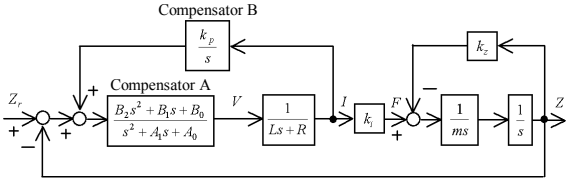

(b) Control system B

FIGURE 4: Block diagram of the control system

EXPERIMENT

Experimental Setup

A photograph of one experimental setup is shown in Figure 3. The displacements of the rotor in the Z and Y directions at the end of the shaft were measured using two capacitance micrometers (MicroSense5504, ADE Corp.) with a measurement range of 0.1 mm, a resolution of 0.15 μm and a bandwidth of 100 kHz. The active region of the displacement sensor probes was 0.5 mm in diameter.

In order to design a controller, the magnetic stiffness k_z in the Z direction, the current-force coefficient k_i, the resistance R and the inductance L of the serially connected coils and the mass of the rotor m have to be known. The measured values of k_z, k_i, R, L and m are -1.8×10^4 N/m, 0.54 N/A, 6.7 Ω, 0.16 mH and 1.3×10^{-4} kg, respectively.

In order to stabilize the MMB, a controller was designed, as follows. A block diagram of the control system is shown in Figure 4. The controller parameters, A_0, A_1, A_2, B_0 and B_1 for control system A (as shown in Figure 4 (a)) were chosen to place all of the closed loop poles at $-2\pi\times7500$ rad/s. A zero power compensator (compensator B) was then added to control system A,

TABLE 1: Controller parameters

Description	Symbol	Value
Multiple-order pole of control system A	p	$-2\pi\times7500$
Parameters of compensator A	A_0	1.4×10^{10}
	A_1	1.9×10^5
	B_0	1.2×10^{16}
	B_1	1.0×10^{12}
	B_2	1.7×10^7
Zero power gain	k_p	0.01

as shown in Figure 4 (b). The zero power compensator works to reduce the offset current to 0 A.

The offset current is induced by the unbalance of the attractive force at the each end of the steel cylinder. The value of k_p for the zero power compensator was determined experimentally by trial and error. The controller parameters are shown in Tables 1. To realize the controller, a digital signal processor (DS1103 PPC Controller Board, dSPACE Inc.) including 16 bit AD and 14 bit DA capability was used. A servo sampling frequency that is a minimum of

ten times greater than the closed loop bandwidth of 7500 Hz, is desirable. However, a servo sampling frequency of 50 kHz was used because the sampling frequency of the digital signal was limited.

Startup Test

The startup responses of the displacement in the Z direction and the coil current are shown in Figure 5. The rotor moved to the center after starting the controller. There is a 5 μm steady-state error due to the zero power compensator and the imbalance of the attractive forces caused by errors in machining and assembly. Although a large current of 1.3 A flows through the small coils just after starting the controller, the coils are not damaged because the large current only flows for a very short period of time and the coil current is within ± 0.1 A during stable levitation.

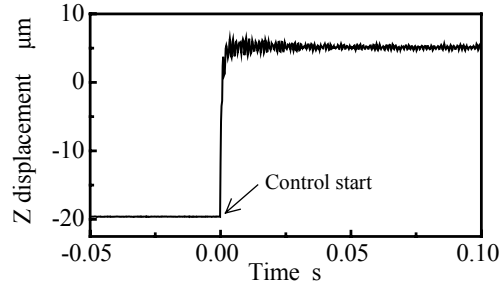

FIGURE 5: Startup responses of the Z displacement and coil current

Magnetic Stiffness

The magnetic stiffness in the passively controlled directions was calculated from the measured natural frequencies of the rigid body modes of the rotor, because the application of any load to the small rotor was difficult to achieve. In order to measure the displacement and the angle in the Y and Θ directions, two capacitance micrometers were arranged in the radial direction at both ends of the shaft. A schematic of the arrangement of the displacement sensors for the measurement of the displacement and the angle in the Y and Θ directions are shown in Figure 6. The natural frequencies of the translational and angular modes,

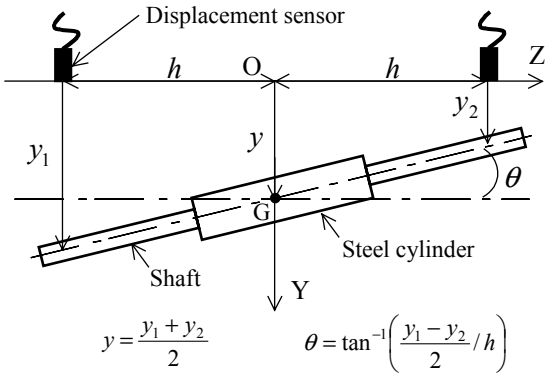

FIGURE 6: Schematic of the sensor arrangement

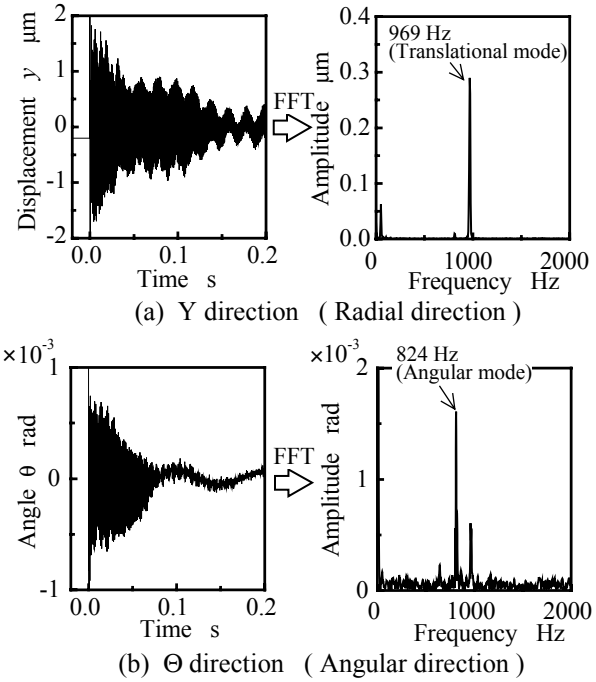

FIGURE 7: Startup response and FFT analysis in the Y and Θ directions

which were 824 and 969 Hz respectively, were measured using the Fast Fourier Transforms (FFT) of the startup responses in the Y and Θ directions, as shown in Figure 7. The magnetic stiffness was calculated using the following equations.

$$k_y = m\omega_y^2$$
$$k_\theta = J\omega_\theta^2 \quad (1)$$

where k_y and k_θ are the magnetic stiffness in the Y and Θ directions, m and J are the mass and the inertia moment about the Y direction of the rotor and ω_y and ω_θ are the natural angular frequencies of the translational and angular modes. The measured magnetic stiffness k_y and k_θ were 4.7 N/mm and 2.7×10^{-2} Nm/rad,

respectively. The simulated magnetic stiffness k_y and k_θ were 3.4 N/mm and 2.0×10^{-2} Nm/rad, which differ from the measured magnetic stiffness due to errors in machining and assembly and the unbalancing effect of the attractive force.

Rotational Accuracy

The rotor could be rotated smoothly by blowing compressed air on to a blade attached to the end of the shaft, as shown in Figure 3. The blade size was 0.7× 2.7 mm. Only one displacement sensor was arranged in the radial direction at the end of the shaft to measure the vibration of the rotor because the blade had to be attached to the other side of the shaft. The output of the displacement sensor arranged in the Y direction includes the displacement of the translational and angular modes. The rotational speed was measured by using the FFT of the displacement sensor output in the radial direction.

The amplitude of the rotor vibration in the radial direction at the end of the shaft is shown in Figure 8 for several speeds. Precession of the vibration with an amplitude of 18 μm may occur at low speed due to machining errors at the edge of the steel cylinder and the pipe edges of the flanges and assembly errors between the shaft and steel cylinder. The amplitude of the vibration increases as the rotational speed approaches the natural frequency of the angular mode of 49,440 rpm. At speeds above 39,000 rpm, the rotor touched the flanges.

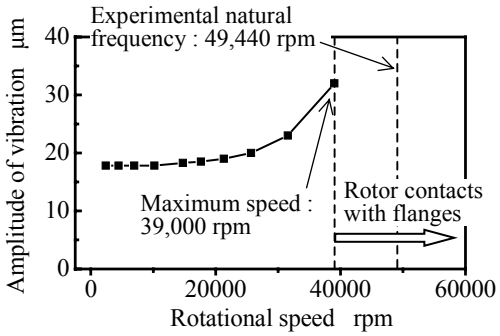

FIGURE 8: Amplitude of rotor vibration (which is measured by one displacement sensor arranged in the Y direction at the end of the shaft)

Power Consumption

The total power consumption of the MMB and the loss in the copper coils were measured at several rotational speeds, as shown in Figure 9. The total power consumption was calculated from the measured coil voltage and the coil current. The copper loss was calculated from the measured coil current and the resistance of the coils. The total power consumption and the copper loss were 20.4 mW and 17.2 mW without rotation, respectively. The total power consumption increases with increasing rotational speed. It can be considered that the power consumption required to control the rotor increases to reduce the rotor vibration induced by the imbalance force. Much of the total power consumption of conventional magnetic bearings can be considered to be due to copper and iron losses. The rotor and electromagnet cores of conventional magnetic bearings are laminated to reduce the iron loss. However, as is evident from Figure 9, the copper loss accounts for much of the total power consumption at a speed of 37,000 rpm, even though a bulk iron core is used for the rotor and the stator of the MMB.

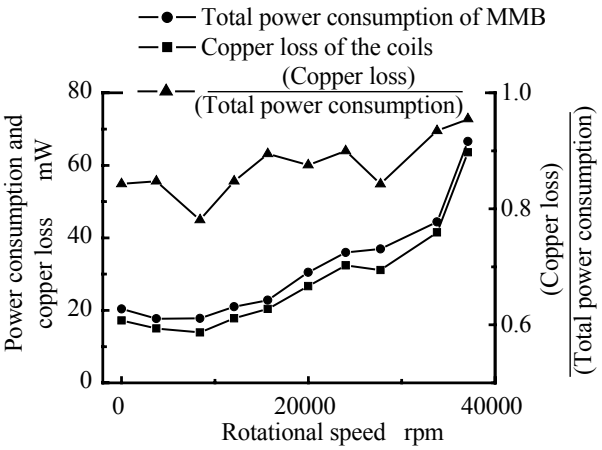

FIGURE 9: Total power consumption, copper loss and the ratio of copper loss to total power consumption of the MMB

Dynamic Characteristics

The frequency response of the MMB was measured using a frequency response analyzer (FRA5095, NF Corp.). A sweep sinusoidal signal with an amplitude of 2 μm was imposed into the desired displacement of the control system. The frequency response $Z(s)/Z_r(s)$ from the desired displacement to the displacement sensor output was measured, as shown in Figure 10.

The MMB was modeled to add the effect of the speed electromotive force to the control system shown in Figure 4 (b). The frequency response was also simulated using the modeled transfer function, with simulated values of k_i and k_z, the measured values of m, L and R shown and the speed electromotive force coefficient k_v, which is assumed to be equal to k_i.

In the experimental frequency response of $Z(s)/Z_r(s)$ at a frequency of 1 Hz, the gain was -40 dB and the phase was 90 degrees, due to the effect of the zero power compensator. Although the effects of the displacement sensor dynamics and the eddy current

were not modeled, even if laminated steel was not used for cores of the rotor and stator, the experimental response approximately corresponds to the simulated values up to a few thousands of Hz. Hence, the simplified model is useful for help in designing the MMB controller.

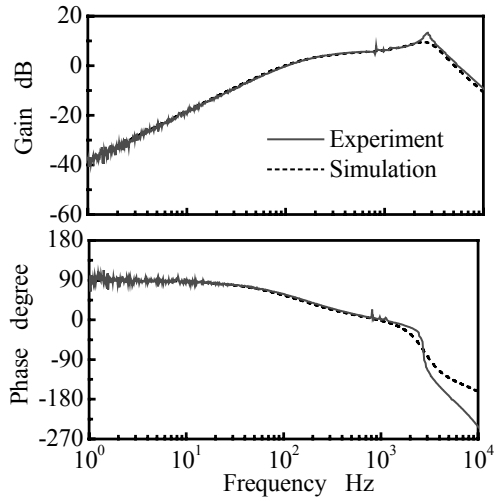

FIGURE 10: Measured and simulated frequency response $Z(s)/Z_r(s)$ from the desired displacement to the displacement sensor output

CONCLUSIONS

A new design was discussed in order to realize an MMB for a 2 mm-diameter rotor. An MMB incorporating only one permanent magnet, two coils and five mechanical parts was fabricated. Stable levitation and smooth rotation of the rotor was verified when using the MMB and the control system. The static and dynamic performances of the MMB were evaluated. The measured magnetic stiffness in the Y and Θ directions was 4.7 N/mm and 2.7×10^{-2} Nm/rad, respectively. The rotor could be rotated at a maximum speed of 39,000 rpm, and the rotor vibration was 18 μm at low speed. The total power consumption and copper loss without rotation were 20.4 mW and 17.2 mW, respectively. The frequency response of the MMB was measured. The MMB was modeled and the frequency response was simulated using the modeled MMB.

In future work, sensor systems will be studied, including the application of sensor-less control of the coils to enable further miniaturization.

ACKNOWLEDGMENTS

This research is partly supported by a Grant-in-Aid for Scientific Research from the Japan Society for the Promotion of Science (JSPS) and the Industrial Technology Research Grant Program in '02 from the New Energy and Industrial Technology Development Organization (NEDO) of Japan.

REFERENCES

[1] Spadaccini, CM., Mehra, A., Lee, J., Zhang, X., Lukachko, S. and Waitz, IA., High power density silicon combustion systems for micro gas turbine engines, *ASME Journal of Engineering for Gas Turbines and Power*, Vol. 125, 2003, pp. 709-19.

[2] Noon, GP., Morley, DL., Abdelsayed, SV., Benkowski, RJ. and Lynchi, BE., Clinical experience with the MicroMed DeBakey ventricular assist device, *The Annals of Thoracic Surgery*, Vol. 71, 2001, S133-8.

[3] Kummerle, M., Aeschlimann, B., Zoethout, J. and Bleuler, H., Acceleration feedforward for increase of bearing stiffness – application for very simple AMBs, *Proceedings of the 7th International Symposium on Magnetic Bearings*, Switzerland, 2000, pp. 141-6.

[4] Yonnet, J., Passive magnetic bearings with permanent magnets, *IEEE Transaction on Magnetics*, Vol. 14, No. 5, 1978, pp. 803-5.

[5] Yonnet, J., Permanent magnet bearings and couplings, *IEEE Transaction on Magnetics*, Vol. 17, No. 1, 1981, pp. 1169-73.

[6] Mukhopadhyay, SC., Ohji, T., Iwahara, M. and Yamada, S., Design, analysis and control of a new repulsive-type magnetic bearing system, *IEE Proceedings - Electric Power Applications*, Vol. 146, No. 1, 1999, pp. 33-40.

[7] Silva, ID. and Horikawa, O., An attraction-type magnetic bearing with control in a single direction, *IEEE Transactions on Industry Applications*, Vol. 36, No. 4, 2000, pp. 1138-42.

[8] Li, L., Shinshi, T., Kuroki, J. and Shimokohbe, A., A one-axis-controlled magnetic bearing and its performance, *JSME International Journal C*, Vol. 46, No. 2, 2003, pp. 391-6.

[9] Kuroki, J., Shinshi, T., Li, L. and Shimokohbe, A., A Micro-Magnetic Bearing Using One-Degree-of-Freedom control, *Proceedings of 7th International Symposium on Magnetic Suspension Technology*, Japan, 2003, pp. 50-55.